ARPN Journal of Engineering and Applied Sciences

HIGH ALTITUDE OPERATIONS WITH PISTON ENGINES POWERPLANT DESIGN OPTIMIZATION PART II: TURBO-CHARGING, TURBO MATCHING, EFFICIENCY AND SERIAL ARRANGEMENT OPTIMIZATION

Luca Piancastelli, Simone Pica and Giampiero Donnici
Department of Industrial Engineering, Alma Mater Studiorum University of Bologna, Viale Risorgimento, Bologna, Italy
E-Mail: luca.piancastelli@unibo.it

ABSTRACT

Low BSFC (Brake Specific Fuel Consumption) and flat-altitude-rating make piston engines ideal choice for altitudes up to 20,000m-65,000ft. These propulsion systems are more complex than traditional applications that are normally limited to 5,000-7,000m (16,000-23,000ft). In fact, the air propulsion (propeller or fan), the air intake, the fuel system, the turbocharging, the exhaust and the cooling system take part to the design optimization process. An integrated design is strictly necessary. At high altitudes, the intake air is taken from high-pressure areas into an alternate, extremely optimized, path. In propeller systems, a diffuser is usually positioned in the lower part of the aircraft. It converts kinetic energy into pressure. In fan systems, a little amount of “high pressure” air is taken from the high-pressure area of the fan. In lower power units, automotive-derived turbochargers can achieve the required pressure ratio. However, this option is limited by the maximum amount of volumetric flow rate. Moreover, automotive turbocharger housings have to be redesigned to use low-weight inconel alloys instead of heavier cast-iron. A complete redesign of the high pressure turbocharger (the unit closer to the engine manifold) can achieve pressure ratios from 8:1 to 10:1. This expensive process increases the power to mass ratio of the propulsion system. For higher power rating over about 200 kW axial compressor-turbine assemblies derived from small turboshafts can be used as a turbocharging unit. In this case the burner is substituted by the piston engine. Especially for diesel engines, the advantage lies in the efficiency (BSFC). In fact, the maximum temperature reached in the diesel combustion chamber is about 4200K and the air flow is much lower than traditional turboshafts. Hybrid and turbocompound solutions are also possible. The exhaust and the intake of the piston engine have to be redesigned. However, the requirements of low weight, high reliability and long endurance HALE (High Altitude Long Endurance) UAVs (Unmanned Aerial Vehicle) requires further work on this specific subject.

Keywords: optimization, HALE, UAV, propulsion, turbochargers, serial cascade arrangement.

INTRODUCTION

Propulsion system is a technical challenge in UAVs designed to fly subsonically >20,000m (65,000ft) for several hours. In this flight regime, TurboChargers (TC) are needed to supply most of the intake pressurization required to compress small air density. Volume flow requirements increase with altitude, which translates to larger TC size. Pressure ratio requirements also increase with altitude, which translates to more TC stages. Since power is proportional to airflow for any air breathing engine, the power plant size required to process airflow for a rated power will grow. Interstage and afterstage cooling is required for efficiency a power output. Weight is proportional to the cube of linear dimensions.

For practical design reasons, beyond certain power levels (≈200kW), the fan replaces the propeller. This choice changes the turbocharger pressure ratio, since already compressed air is present inside the fan. Because of the increased size and weight of the air handling system and thrust delivery components, a propulsion system optimized for high altitudes is significantly larger and heavier than its low altitude counterpart. Moreover, the HALE (High Altitude Long Endurance) vehicle needs more power to stay aloft. In fact, faster flight speeds are necessary to maintain dynamic pressure and support its weight in low-density air. Therefore, the propulsion system claims greater fractions of the airplane's gross weight. This runs counter to the airplane's ability to carry the necessary fuel weight and payload. In this second part of the paper, the turbocharging system options are discussed.

In small piston engines engine, intake pressurized with two or three cascaded stages of turbocharging is a best choice for next generation of high altitude atmospheric science aircraft. This paper presents the four available options: diesel-propeller, diesel-fan, spark-ignition propeller and spark-ignition fan, which are discussed and compared in the context of the flight regime. Unsurprisingly, piston engines compares favourably with the turbofans in the small power plants. Finally, an example is made for a spark ignition piston engine.

The mission

Since the fuel consumption follows a cubic low with speed, long endurance requires flying at reasonably

ARPN Journal of Engineering and Applied Sciences

low speeds. The dynamic pressure available limits the minimum speed to about 0.4M.

Therefore, the aircraft will be more like a sailplane than a powered aircraft and will face handling problems at take off and lower altitudes.

The propulsion challenge

It should be acknowledged that the propulsion challenge is not so huge that it may appear. In fact, short 15 years after the Wright brothers made their historic flight; General Electric entered the annals of aviation history by installing an exhaust-driven turbocharger to a Liberty engine and tested it at about 4,000m. There, the 350 HP a.s.l Liberty engine outputted a remarkable 356 HP instead of the mere 240HP of the naturally aspirated engine. In fact, Macready makes the altitude record at 11,800m three years later. Mario Pezzi with his supercharged Caproni achieved a world record of 17000m in 1938. Serial production B-17 and B-29 bombers along with the P-38 and P-51 fighters were all fitted with turbochargers with partially automated controls. In the automotive market, much of the early developments in turbocharging came as a result of demands from the heavy duty diesel engine market. It wasn't until the mid-1980s that this technology was seriously applied to diesel and spark ignition cars. Turbocharging is then a fairly mature technology both for the aviation and the automotive industry. On the turbine side the history is more recent. At lower altitudes, typically 10,000m, the turbine engine can generate up to 5 times higher power density than the reciprocating engine, as long as inlet air mass flow is adequate. In turbines, airflow cools down the engine and the mass flow is significantly higher than in piston engine with the same power rating. Mass flow is achievable at normal altitudes by flying at faster speeds using inlet pressure recovery. Historically the turbine engine was premium choice to high altitude flight, since it was the first serial-production power plant with high enough specific power to push level flight into the supersonic range. The turbine engine significantly higher fuel consumption, up to 5 times that of the piston engine, is not a major disadvantage for aircrafts because of the higher specific power.

The GE-J79-3 powered, AQM91 Compass Arrow spy plane achieved better than 25,000m in 1969.

This aircraft achieved this record altitude flying at M = 0.83, the limit speed necessary to give the inlet pre-compression needed to keep its combustor lit. This turbojet engine exhibited a specific thrust that was approximately proportional to ingested air density since machine size is fixed. Combustor pressure drops off as density decreases with altitude. In fact, the machine ingests the same air volume, but thrust depends on air mass.

The limit is the point where combustion of fuel is operating on the verge of flameout. Figure-1 shows the J97's thrust curve, whose behaviour is typical of turbojet and turbofan engines. The thrust of the Compass Arrow's J97 turbojet was 825N/0.85M at 24,000m with a reduction of 95% from the sea-level-trust.

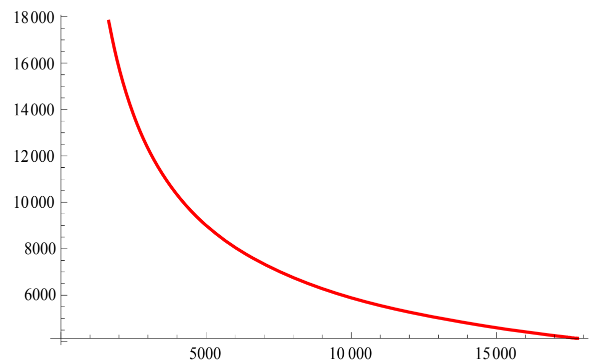

Figure-1. Compass Arrow's J97 Altitude (m) vs. Thrust (N).

Engine comparison

The weight penalty associated with air handling and thermal management becomes the major discriminator when choosing engine for a HALE. There are three candidates to consider: turbines, spark-ignition and diesel turbocharged reciprocating engines. Propeller, fan and jet are available as thrusters. However, propellers find their upper limit at about 200kW, while jet propulsion is unfeasible with piston engines.

Fan-engines are installed in very large high-speed subsonic aircrafts (0.7<M<0.95) with wing loadings in the range of sailplanes (500-1500Pa); the propeller- engines power slower aircraft (0.4<M<0.6) with even lower wing loading (100 -500 Pa). An overall pressure ratio better than 19:1 is necessary to recover the s.l. density at 20,000m.

Intake pressurization requires up to 3 centrifugal compressor stages. Because of low inlet density, the first turbomachinery is large in size. Commercial centrifugal turbochargers availability limits the maximum displacement of piston engine possible. Equations (1) (2) and (3) make it possible to evaluate the displacement of the engine for a given compressor map (4).

$$p = p_b e^{\frac{g(H-H_B)}{RT_B}} \quad H \in \{11000{,}20000\} \tag{1}$$

Equation (1) is the ISA barometric pressure from 11,000m up to 20,000m.

$$r = \frac{p_0 + Boost}{r_{inlet}\, p} \tag{2}$$

Equation (2) is the pressure ratio with the dynamic (ram) air inducer recovery ratio (r_{inlet}).

ARPN Journal of Engineering and Applied Sciences

$$CFR = 0.069 \frac{V_{cc} rpm\, \eta_e}{16.39\tau 1728} r \frac{\sqrt{\frac{T_r}{545}}}{\frac{p_{0\_psi}}{13.95}} \tag{3}$$

Equation (3) is the classical Corrected Flow Rate (CFR) equation with the conversion factors. This equation does not hold for stratospheric flight. In fact, it uses the standard air density to convert the volumetric flow into a standard mass flow. When the compressor is tested, the flow rate is corrected for standard conditions (13.95psi and 545 F absolute) which corresponds to the standard air density. The standard air density is 0.069 lb/ft^3 or 1.10 kg/m^3. The correction is the same that converts the BFR into the CFR (4).

$$CFR = BFR \frac{\sqrt{\frac{T_r}{545}}}{\frac{p_{0\_psi}}{13.95}} \tag{4}$$

The compressor uses a normalized mass flow instead of the volumetric flow rate. If the TC works in the classical automotive environment the method holds. Equation (4) converts the outside into standard air. The standard mass flow corresponds to a standard volumetric flow. Reynolds and Mach number are within tolerance and the manufacturer compressor maps are valid for car and trucks. For stratospheric use the equations (3) and (4) need more accurate corrections.

The compressor and the piston engine work with volumetric flows. Fuel injection works with mass flow. The power output depends on fuel quantity, fuel specific energy and efficiency. In normal turbocharged piston engines, the turbomachinery compresses the outside air. Then, the aftercooler cools the air at a temperature lower than 50 DEG C. This temperature is linked to knocking limits for spark-ignition engines and to cooling for CRDIDs (Common Rail Direct Injection Diesel). Above 50 DEG C, the output power of the piston engine will be reduced by the FADEC. Then, the piston engine aspirates the compressed air in the intake. This compression is then closer to an isothermal than an adiabatic one. In fact, it starts from OAT (Outside Air Temperature) and ends at manifold aftercooler-exit-temperature (50 DEG C maximum).

In the stratosphere, the standard OAT T_r is -56.5 DEG C (390.3 F absolute). The engine aspires a volumetric flow rate at intake temperature and pressure. This is given by equation (5).

$$BVFR_m = \frac{V_{m3} rps\, \eta_e}{\tau} \tag{5}$$

The corresponding density at the intake is (perfect gas law) (6):

$$\frac{p_{intake}}{\rho_{intake}} = RT_{intake} \Rightarrow \rho_{intake} = \frac{p_{intake}}{RT_{intake}} \tag{6}$$

The mass flow rate BFR_m (7) at the engine intake is almost equal to the mass at every TC intake (cascade arrangement-single TC per stage). Actually OA flow rate it slightly larger due to blade gaps that recirculate a small quantity of air.

$$BFR_m = \frac{V_{m3} rps\, \eta_e}{\tau} \rho_{intake} \tag{7}$$

Due to the assumption of the conservation of the mass flow, the volumetric OA (Outside Air) flow rate $CBVFR_m$ is (8):

$$CBVFR_m = \frac{V_{m3} rps\, \eta_e}{\tau} \frac{\rho_{intake}}{\rho_{OA}} \tag{8}$$

Since the perfect gas law holds, equation 8 can be rewritten as (9).

$$CBVFR_m = \frac{V_{m3} rps\, \eta_e}{\tau} \frac{p_{intake} T_{oa}}{p_{OA} T_{intake}} \tag{9}$$

The standard mass flow of the compressor map is a volumetric flow in standard conditions. To be more accurate, since the Garrett standard air is different from ISA atmosphere standard a conversion can be made by using equation (4). In this case, the ISA+0 a.s.l. give the correction factor: T*r*=59+460 (F absolute) and p0_psi=14.6959 (psi). Equation (4) becomes then equation (10).

$$CFR = 0.069 \frac{V_{cc} rpm\, \eta_e}{16.39\tau 1728} r \frac{\sqrt{\frac{59+460}{545}}}{\frac{14.6959}{13.95}} \tag{10}$$

Equation (10) can then be updated with the pressure ratio r defined by the density ratio. The "altitude pressure ratio" r is then (11):

$$r = \frac{p_{intake} T_{oa}}{p_{OA} T_{intake}} \tag{11}$$

and equation (10) becomes (12). This new CFR is the one of Garrett maps (Figure 2).

VOL. 11, NO. 7, APRIL 2016 ISSN 1819-6608
ARPN Journal of Engineering and Applied Sciences

www.arpnjournals.com

$$CFR = 0.069 \frac{V_{cc} rpm\, \eta_e}{16.39\tau 1728} \frac{p_{\text{int}ake} T_{oa}}{r_{inlet} p_{OA} T_{\text{int}ake}} \frac{\sqrt{\frac{59+460}{545}}}{\frac{14.6959}{13.95}} \qquad (12)$$

However, the impact of the low Reynolds number conditions at altitude on the performance of small centrifugal compressors is relevant. The reduction in Reynolds number at high altitude leads to a certain loss in compressor efficiency. At 20,000m compressor efficiency is lowered by up to 10% at the design point (maximum efficiency) rotational speed. At 50% of the design rotational speed the efficiency loss can reach 15% at 20,000m. This is due to the significantly lower operational Reynolds number at low rotational speeds.

Under off-design operation, the loss in efficiency is more important for smaller automotive compressors than larger ones. This loss in efficiency with altitude is negligible in the troposphere (11,000m). In the stratosphere it starts to increase rapidly.

Altitude also leads to a small loss in pressure ratio at a given rotational speed. Pressure losses of around 5% are common for the design rotational speed at 20,000 m.

The thicker boundary layer at low Reynolds number conditions and the lower Mach number lead to a reduction in maximum mass flow rate capacity at compressor choke.

The surge line is not as marked as a.s.l. and slower transition to surge is associated to thinner air.

The efficiency loss in both compressor and turbine will drive operation of the engine to higher turbine inlet temperatures. Therefore, the largest turbine which is available from the TC manufacturer is more convenient for high altitude operations. Updated compressor maps are necessary for simulation of altitude performance of piston engines. CFD (Computational Flow Dynamic) simulation can effectively redraw these maps. Another problem is that the efficiency curves have local minimums that will affect TC cascade operation. The TCs will run at different velocities at the same altitude depending on the mission history. To avoid this problem every TC should be controlled with a wastegate. In the stratosphere the temperature T_{OA}=-56.5 DEG C and T_{intake}=50 DEG C are fixed.

It is then possible to calculate the maximum engine displacement for a certain low-pressure TC flow rate (lb/min) (10).

$$Vcc = \frac{1.32\times10^6 e^{\frac{g(H-H_b)}{T_b R}} r_{inlet} p_b CFR}{\eta_e (Boost+p_0) rpm} \qquad (10)$$

For example, the largest turbocharger on Garrett Catalogue (GT6041, Figure-2) can process, at maximum pressure, a corrected airflow of 160 lb/min.

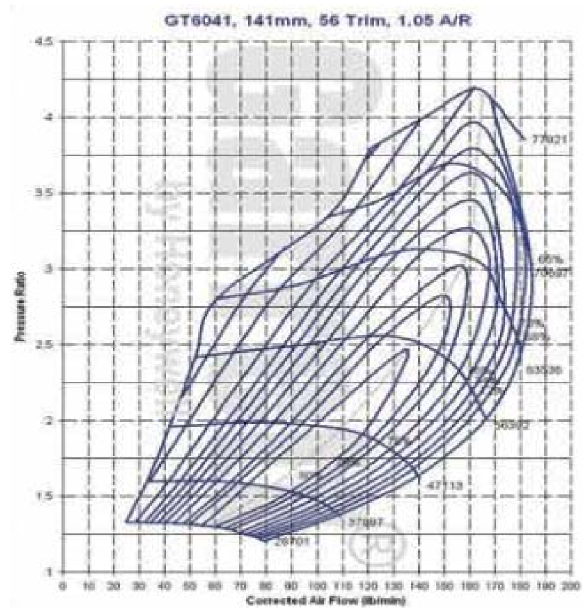

Figure-2. GT6041 map.

The maximum displacement is about 2, 400cc@20,000m. In fact, a typical naturally aspirated spark ignition piston engine will require a slight overboost to operate at 50 DEG C air intake temperatures. In fact, normally, brake tests are performed at 25 DEG C. The air density loss is recovered with approximately 8500 Pa boost (11). However, temperature increases the knocking and the reduction in time advance increases Specific Fuel Consumption (SFC).

$$boost_{nb} = \frac{T_{boost} p_0}{T_0} - p_0 = 8500$$
$$\Rightarrow r_{nb} = \frac{T_{boost} p_0}{T_0 p_0} = 1.085 \qquad (13)$$

Therefore, the engine compression ratio is also slightly reduced to avoid knocking with the original advance. An additional metal sheet is added to the metal head gasket to obtain this result. A continuous allowed rpm is 5,500rpm and a reasonable volumetric efficiency is 0.83. Normally 200HP are available from a naturally aspirated piston engine with 2,400cc displacement. If a CRDID is used, a reasonable boost is 1.6bar and the volumetric efficiency is about 0.81 at 3,800rpm. In this case, the maximum displacement is 1,200cc. No modifications are required to the engine, since the CRDID are always turbocharged. In this case, if two Garrett 6041 TCs are used the power is about 300HP. Therefore, spark-ignition and diesel engine have approximately the same power output. The difference is that the diesel has a far better SFC (minus 40% at full load), while the spark ignition engine can reach higher altitudes. In fact, the

VOL. 11, NO. 7, APRIL 2016 ISSN 1819-6608
ARPN Journal of Engineering and Applied Sciences

www.arpnjournals.com

CRDID will shut down when the peak pressure inside the combustion chamber fades under 80bar. Heating can be used to keep the CRDID working, like a bypass in the aftercooler or intake heating (for example by using the exhaust gas), but these devices will reduce SFC. Moreover, the diesel specific power is lower, since the engine and the turbomachinery are heavier. Diesel is convenient only for endurance and safety when heavy fuel is used.

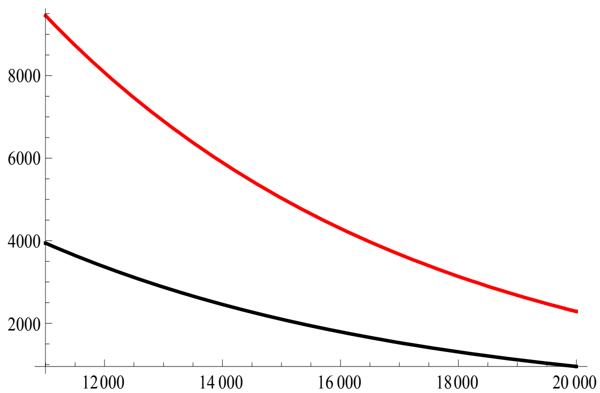

Figure-3. Maximum engine displacement (cc) vs altitude (m) RED is turbo-normalization, BLACK is Boost=1.6bar for Garrett GT6041 (ram air intake).

The displacements of Figure-3 hold for a ram air inducer with a compression ratio of 1.05. This is typical of a propeller aircraft. If a fan is used, the inducer takes air from the high-pressure area of the fan is a compressor ratio of 1.3. Figure-4 gives the maximum displacements in this case.

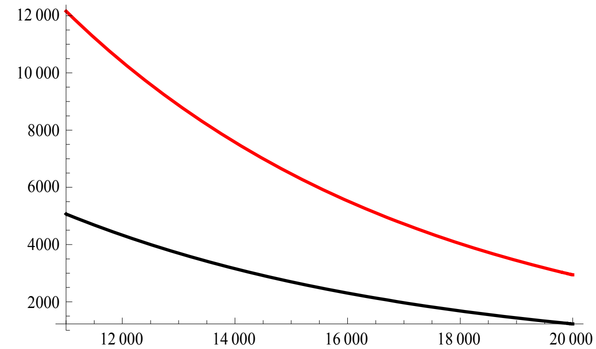

Figure-4. maximum engine displacement (cc) vs altitude (m) RED is turbo-normalization, BLACK is Boost=1.6bar for Garrett GT6041 (fan air intake).

The diesel maximum displacement is then about 1, 900cc. In this case, it is possible to obtain 200HP (147kW). The naturally-aspirated spark-ignition fan-engine has a displacement of 3000cc and a power output of 260HP. The power advantage with the fan is then marginal, so the reciprocating engines seems to be best matched with propellers, at least if you use commercial turbochargers.

In fact, flying subsonically in low-density air also creates the requirement for larger thruster "actuator disk" area in order to achieve optimal propulsive efficiencies that are fundamental to reduce fuel consumption and provide range. In general, 0.9M is the approximate upper speed limit for a subsonic jet/fan aircraft, while Mach 0.4 represents the minimum reasonable aircraft speed for a propeller. Therefore, for range and endurance a propeller is more efficient than a fan.

Cost effectiveness

The reciprocating engine is the most cost-effective, because of the existing technology base of mass produced automotive units that can be adapted to build a high altitude reciprocating engine. Recent trends in automobile manufacturing tend to reduce weight to improve fuel economy. Therefore, the new engines have rendered the automotive technology base even more convenient for aircraft propulsion, to the extent that a few manufacturers have developed automotive powerplant conversions that are extremely weight competitive with certified aero engine installations. The autoracing marketplace for turbocharged engines already includes a number of small business developers who mainly modify and assemble hardware manufactured by others. The turbocharged powerplant is then cheaper because it is built up from mass produced components. The development costs are also reasonable, because there is a considerable design heritage that survives from pre-turbine age aviation, and from the experience gained from earlier attempts to develop turbocharged high altitude powerplants. A few multiple stage turbocharged systems

ARPN Journal of Engineering and Applied Sciences

www.arpnjournals.com

have already been tested in high altitude flight or altitude test chambers.

Table-1. High altitude performance of high altitude vehicles powered by turbocharged piston engines.

	Engine (cc)	**#stages**	**HP** (km)	**Chamber max** (km)	**Flight max** (km)
Caproni Ca 161bis	18000	1	750 (7.5)	-	17
Teal Rain	2x1211	3	2x70 (20)	20	-
Condor	2x5800	2	2x182 (20)	22	20.4
Strato 2c	2x9000	Axial Cent.	2x400 (23)	24	18.5
Raptor	1211	2	103 (16)	21	18
Perseus	1211	3	73 (18)	18	18
Altus	1211	2	103 (16)	21	17
Erast	1211	3	100 (23)	20	-

Table-1 shows a few maximum performances achieved by spark-ignition turbocharged reciprocating engines. At normal altitudes, the power density of a turbine is higher than the reciprocating engine one. The piston engine begins to compare favourably with turbine engine at altitudes above 11,000m when low speeds favour long range and endurance. In fact, at low speed the inlet pre-compression is limited. In this case, multiple stages of turbocharging achieve the necessary compression for atmosphere pressure and density compensation. The mass grow rate of piston engines with altitude is not as high as the turbines. In piston engines, the turbocharging compresses only the induction air, which is less than 1/10th the turbine air consumption.

In this contest, the spark-ignited engines have the highest altitude potential due to the nearly stochiometric fuel air mixture, that minimize the induction airflow. As multiple stage units arranged in cascade pressurize the intake air, the increased pressure ratio of the TC turbines increases enthalpy extraction efficiency, fully balancing the compressor work. The excess of turbine power available can be usefully transformed in thrust through the exhaust. However, a better option is to improve the efficiency of the cooling duct. This will reduce the radiator size, which is critical in high altitude operations. In fact, radiator size depends essentially on air density.

Above critical altitude, the compressor of the TC cannot maintain the intake pressure, so the power curve exhibits a lapse behaviour similar to the turbojet. To reduce powerplant mass and volume (drag) the critical altitude coincides with or is slightly lower than the aircraft's design altitude.

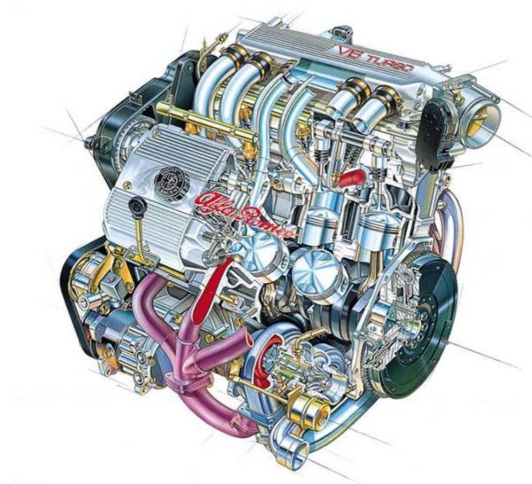

Figure-5. The latest (year 2000) V6-60° 3L Busso Engine.

General consideration on turbocharging

The manufacturers of commercial centrifugal TCs optimize the system. Optimization consists in optimal design and matching of turbine and compressor. With modern CFDs compressor impeller and turbine wheel optimization is not as critical as it was previously. However, the inlet, the diffuser and the collector design of the compressor are still problematic. For automotive applications, it is very important to widen as possible the map in terms of airflow and to reduce the TC volumes and inertia to reduce the turbolag. In aircraft design, the turbolag is not important and the collector and diffuser volume can be larger to increase pressure ratio. However, the costs of this operation are important, since experimental tests are strictly necessary. Turbolag minimization is the most important parameter in automotive centripetal turbine optimization. Turbine wheel under sizing is common to reduce polar inertia. A larger wheel, if available from the manufacturer is then

ARPN Journal of Engineering and Applied Sciences

more effective in aerial applications. The optimization of the most effective exhaust configurations of turbocharging system is extremely important. In fact, turbochargers and engine performances are greatly affected by the gas flow unsteadiness. Four different systems are available: the Constant Pressure turbocharging system (CP), the Pulse Turbocharging system (PT), the Pulse Converter (PC) turbocharging system and the Modular Pulse Converter (MPC) turbocharging system. In the CP turbocharging system the exhaust gases coming from all cylinders flow into a common exhaust manifold, whose volume is sufficient to damp down the unsteady flow, and then feed the single-entry turbine. The CP system keeps the pressure at the turbine entry steady with time, providing a nearly constant pressure turbocharging. As the mass flow is relatively constant, the turbine achieves high efficiency. The disadvantage of this kind of turbocharging system is that a large part of the high kinetic energy of the exhaust gases is lost and the relative large volume increases the mass of the system. Moreover, the turbulence losses, due to the mixing process between exhaust flows, coming from different cylinders, decrease the available energy. The major advantage of CP at intake and exhaust is that the turbine is, theoretically, at its best efficiency. In fact, both the turbine and the compressor are basically quasi steady flow machines, with surge and choke lines that are drawn in the steady state condition. A better utilization of the exhaust kinetic energy is achieved by adopting the PT system, in which the converted energy at the turbine is larger than the CP system. However, the turbine efficiency and flux stability are lower because the gas flow into the turbine is highly unsteady and the turbine operates under variable conditions. The grouping together of several cylinders in a common exhaust pipe reduces the flow unsteadiness. A Pulse Converter (PC) completes the PT system. The disadvantage of PC is that the structure of the exhaust manifolds is complicated, but the mass and volume is reduced from the CP system. Therefore, PT-PC is widely used in the exhaust-turbine side, while the CP system is more common in the compressor/engine-intake side. Specialized software optimizes the intake volume and geometry. An air filtering system is advisable at take-off. For this reason, a “low-altitude” alternate system is designed for near ground operations. This system feeds the first turbocharging system with the aftercooler. For “high-altitude” operations, an alternate inlet converts speed into pressure. An air inlet is located into a high pressure area of the aircraft. Then, a trumpet diffuser converts velocity in pressure and feeds the first compressors at altitude. Typically a subsonic inlet will have a recovery pressure ratio of 1.05. In fan propelled aircraft the inlet takes air from the fan high pressure area and the pressure recovery is about 1.3. The FADEC controls the transition from s.l. to altitude turbocharging systems through electronically operated butterfly valves on the compressor side. This system also controls the overboost. Unfortunately, it is also necessary to install electronically operated wastegates on turbines to avoid TC overspeed and to operate the single TC at a high efficiency point. In fact, automotive turbochargers operated at altitude may have several local maximum of efficiency points. Luckily, modern automotive TCs usually have the possibility to install an electric actuator on the wastegate that is usually included in the TC. Since overheating is possible, titanium alloys are common in impeller of TC compressors. For economic reasons the automotive turbine housings are made of cast-iron. These housings are usually substituted with Inconel or aluminium alloy ones. The aluminium alloy casings are liquid-cooled. An electrical, additional lubrication pump avoids oil cracking in the low pressure TCs during climb. Ball bearing TCs are more expensive and less reliable than fluid film ones. Theoretically, the exhaust section of the turbocharging system is more critical than the intake one for best efficiency. Practically, the high temperature exhaust gases have more energy than needed. In traditional application, an ejector exhaust converts the residual energy into thrust. However, the installation requirement that should minimize the volume and the mass is more important than the additional thrust. Typically, the turbocharging system design aims to minimum volume and mass. Usually a reduction of efficiency is associated to turbine and compressor operations at the lower Reynolds number typical of high altitude flight. For this reason the highest pressure turbine before the aftercooler is substituted with and high temperature unit. The limit operating temperature of commercial TC turbines is about 1300K.

An example: turbocharging the Alfa Romeo Busso spark-ignition engine (Table-2)

Table-2. Busso engine data.

Data	Value	Unit
Displacement	3000	cc
Volumetric Efficiency	0.88	
Max. continuous power	226	HP
Max. continuous speed	4500	rpm
Max speed	9000	rpm
BSFC@4500rpm	196	gr/HPh
Dry Weight	128	kg
TBO@4500rpm	1000	h

Alfa Romeo Busso V6 engine would eventually range from 2.0 L to 3.2 L displacement. With modifications, it is possible to increase engine displacement to 3.8 L. In the early 1970s Giuseppe Busso developed the original SOHC (Single Over Head Camshaft) 12-valve design. In 1993, the first DOHC (Double Over Head Camshaft) version of this engine appeared powering the Alfa Romeo 164. The engine is a racing designed, aluminium alloy block/head with sodium filled exhaust valves. The 3.0 L engine began production

ARPN Journal of Engineering and Applied Sciences

in 1987. This engine was upgraded to dual overhead cams and four valves per cylinder (DOHC-24-valve) in 1993. Due to this and other refinements, this engine produced 229HP (171 kW) up to Euro 4 pollution standards. The Busso engine is lightweight (128kg without alternator in this version, down to 110kg without clutch). It is also extremely sturdy, being able to run at full load at 4,500rpm for 1,500h. Figure-4 shows the performance curves of this engine in the "Euro 0" version. The 3L version is the most suited for aerial vehicle, since 3.2L and 3.8L have a longer stroke with advantages in low speed torque but penalties in high-speed durability. The aeronautical 3L can use cams that are far from ideal for automotive use, in which high torque at low speed is optimized. Many racing derived components are available for this classic engine: FADECs, strengthened pistons, titanium alloys components, racing carbon clutches, lightweight intake and exhausts… These components are easily adaptable for aircraft use.

The output power at 4,500rpm at full load (throttle) is 226HP (166 kW). The engine was the first to use platinum spark plugs that last over 1,000h. The spark plugs take a run-in to eliminate infantile failure that is typical of these components. Therefore, spark plug reliability is over 1/100,000 in 1,000h. A timing belt, which can also last the TBO of the engine, drives the cams. Maintenance consists of oil and filter replacement every 400h. The worn out engine at the end of the TBO will consume at most 1kg of oil every 15h. Treatments on liners and camshafts can extend the initial TBO of 1,000h three-folds.

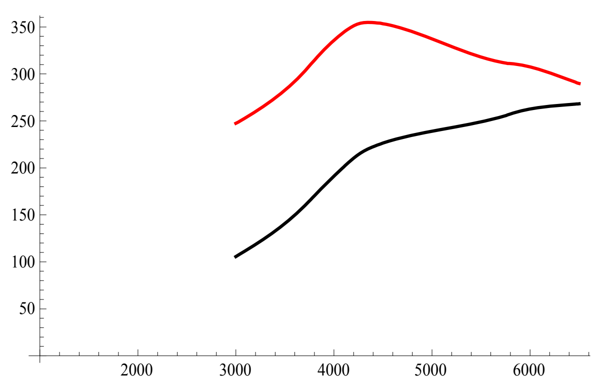

Figure-6. Power (HP-black) vs. Torque (Nm-rpm) vs rpm for the latest Busso Euro 0.

Turbocharging the Busso engine for 20,000m critical altitude

The turbomatching process starts from the lower pressure turbocharger that will compress air at the cruise altitude and will provide it to the second TC through the intercooler. Figure-7 shows the map of the largest turbocharger available from Garrett catalogue: the GT6041. A reasonable inducer recovery pressure ratio is r_{inlet}=1.05.

The Busso engine "mass flow" CFR=172lb/min requirement at 20,000m density altitude is calculated through equation 9. The compression ratio at this flow rate is about 4. The air will then enter into the compressor at $p20000/r_{inlet}$=5748 Pa and will exit at 22,900 Pa (10,925m). The temperature rise is about T_r=114 (6) DEG C and the exit temperature is 60 DEG C (14).

$$T_r = -32 + T_i\left(\frac{PR_i^{0.28}-1}{\eta_c}\right)\frac{5}{9} = 114 \tag{14}$$

An intercooler is necessary to protect the second stage from overheating with the standard aluminium alloy impeller. To avoid the intercooler a titanium alloy can be used for the second stage impeller. It is also possible to calculate at which density altitude the CFR of the Busso Engine at 4,500rpm is in the map (CFR≅30 lb/min). This altitude is about 7,000m. However, at this density altitude, another compressor is still working. An overlap is then present. The remaining PR is (P0+boost)/ P_{Istage}≅4 that is excessive for a single "small" commercial turbocharger. In fact, altitude reduces the s.l. compression ratio. It is then better to use three stages compression. The total compression ratio is PR=19.1. Therefore the single compressor would provide $PR_{singlestage}$=PR^(1/3)=2.67. The input pressure to the intermediate TC is then OAP*P $PR_{singlestage}$*r_{inlet}=15,336 Pa that corresponds to a pressure altitude of 13,468m.

An efficiency of 75% is reasonable for the GT6041at this compression ratio. The temperature rise will then be of 69 DEG C (14) for an inlet temperature at the second (intermediate pressure) TC of about +3 DEG C and a density of 0.19 kg/m^3.

Theoretically with three turbochargers also the intermediate compressor can keep the original aluminium alloy impeller. However, for the local maximum of the efficiencies, it is better to use a titanium alloy impeller.

Equation (12) outputs the standard flow for the Garrett maps of about 80 lb/min. The right Garrett TC is then the GT5533R.

ARPN Journal of Engineering and Applied Sciences

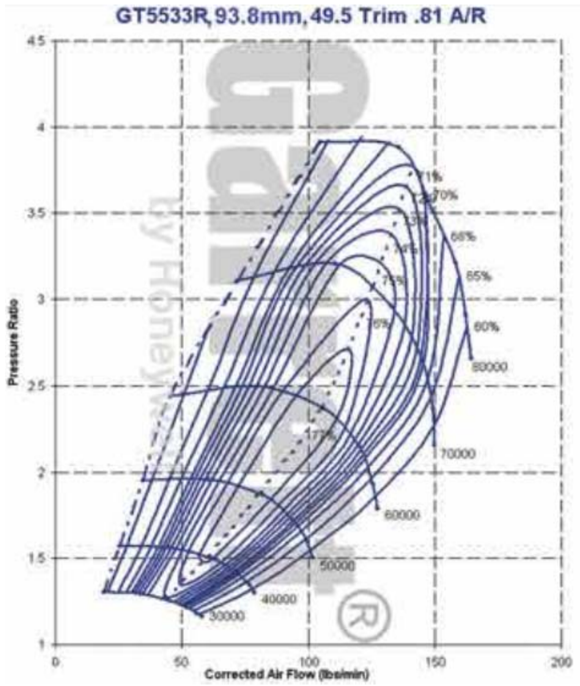

Figure-7. Intermediate TC compressor map.

Again an efficiency of 75% is reasonable for the GT6041at 2.76 compression ratio. The pressure is OAP*($PR_{singlestage}$)^2*r_{inlet}= 43,790Pa. The pressure altitude is 6,540m. The exit temperature is 98°C and the density is $\rho_{intermediate}$=0.41 kg/m^3. It seems to be convenient to use an intercooler. Equation (15) outputs the pressure drop in the intercooler.

$$\Delta p = \frac{v^2}{2}\xi\rho \tag{7}$$

Since the velocity v inside the intercooler is approximately constant, the pressure drop is proportional to air density.

At a boost of 2 bar (303,975 Pa absolute pressure, PR≈3) a typical pressure drop is 2 psi≅14,000 Pa. The pressure drop at 43790Pa absolute pressure is then proportional to $\rho_{intermediate}/\rho_{Garrett}$ = 0.37. Therefore, it is about 5,000Pa. The output pressure from the intercooler is then about 39,500Pa. Part III of this paper will contain a more detailed description of the high altitude cooling systems. At intercooler outlet the temperature will be 10°C and the density 0.45 kg/m^3**.**

The GT2867R seems to fit the 33.42 lb/min requirement (12). A titanium alloy impeller for the compressor is the best choice for reliability. In this case, since turbine efficiency drops with temperature, it is necessary to use a high temperature turbine wheel with 1300K limit.

CONCLUSIONS

Turbocharged diesel and spark-ignition piston engines are a possible choice for long endurance, high altitude operations (10,000m/33,000ft) and extremely high altitude operations (20,000m-65,000ft). In fact, piston engines SFC (Specific Fuel Consumption) is independent from altitude. However, these propulsion systems are more complex than traditional ones that are normally limited to 5, 000-7, 000m (16, 000-23, 000ft). In fact, the air-side propulsion system (propeller or fan), the air intake, the fuel system, the turbocharging, the exhaust and the cooling system take a more important than in traditional “power pack” systems. An integrated design is strictly necessary. At high altitudes, the air is taken from high-pressure areas into an alternate, extremely optimized, path. In propeller propulsion systems, the induction system diffuser converts the air kinetic energy at cruise into pressure. In fan systems, a little amount of “high pressure” air is taken from the high-pressure area of the fan. The air is then ingested by the lowest up to the highest pressure turbochargers that are arranged in cascade. Commercial automotive turbochargers limit the maximum power output possible to about 200HP. Over this value, a turboshaft compressor-turbine assembly is the easier option. In this case, the piston engine replaces the turboshaft burner as in the STRATO 2c prototype. Automotive derived map are to be redrawn through CFD simulation to match the lower Reynolds number and Mach speed of the stratosphere. Intercoolers size is proportional to the inverse of air density. Local efficiency maximums require the installation of blow-off and wastegate valves controlled by engine FADEC.

REFERENCES

[1] Wolfer H. Ignition Lag in Diesel Engines VDI-Forchungsheft 392, 1938, (English Translation, RAE Farnborough, Lib. No 359, UDC 621-436 - 047, Ig5g).

[2] E Mancaruso, S. S. Merola, B. M. Vaglieco. 2008. Study of the multi-injection combustion process in a transparent direct injection common rail diesel engine by means of optical techniques. International Journal of Engine Research (Impact Factor: 0.52). 01/2008; 9(6):483-498. DOI: 10.1243/14680874JER01308.

[3] H. Bettes. 2003. Flow bench applications and techniques, Superflow.

[4] Kalitzin G. and Iaccarino G. 2002. Turbulence Modeling in an Immersed-Boundary RANS-Method, Center for Turbulence Research Annual Research Briefs, Stanford University, California. pp. 415-426.

[5] Shuvom G. 2011. Practical Flow Simulation at Highway Speeds. http://blog.capinc.com/2011/06/practical-flow-simulation-at-highway-speeds/.

[6] Franke R. 1982. Scattered data interpolation: Tests of some methods. Math. Comput. 38, 181-200.

[7] Ferziger J. H. and Peric M. 2002. Computational Methods for Fluid Dynamics. Springer-Verlag, third-edition.

[8] Lam C. K. G. and Bremhorst K. A. 1981. Modified Form of Model for Predicting Wall Turbulence. ASME Journal of Fluids Engineering. 103: 456-460.

[9] Wilcox D. C. 1994. Turbulence Modeling for CFD. DCW Industries.

[10] L. Piancastelli, L. Frizziero. 2014. Turbocharging and turbo compounding optimization in automotive racing. Asian Research Publishing Network (ARPN). Journal of Engineering and Applied Sciences. ISSN 1819-6608, 9(11): 2192-2199, EBSCO Publishing, USA.

[11] L. Piancastelli, L. Frizziero, G. Donnici. 2014. The common-rail fuel injection technique in turbocharged di-diesel-engines for aircraft applications. Asian Research Publishing Network (ARPN). Journal of Engineering and Applied Sciences. ISSN 1819-6608, 9(12): 2493-2499, EBSCO Publishing, USA.

[12] L. Piancastelli, L. Frizziero. 2015. Supercharging systems in small aircraft diesel common rail engines derived from the automotive field. Asian Research Publishing Network (ARPN). Journal of Engineering and Applied Sciences. ISSN 1819-6608, 10(1): 20-26, EBSCO Publishing, USA.

[13] L. Piancastelli, L. Frizziero. 2015. Accelerated FEM analysis for critical engine components. Published by Walailak Journal of Science and Technology The Walailak Journal of Science and Technology, Institute of Research and Development, Walailak University, ISSN: 1686-3933, Thasala, Nakhon Si Thammarat 80161. 12(2): 151-165, Thailand.

[14] L. Piancastelli, L. Frizziero, G. Donnici. 2015. Turbo matching of small aircraft diesel common rail engines derived from the automotive field. Asian Research Publishing Network. ARPN Journal of Engineering and Applied Sciences. ISSN 1819-6608, 10(1): 172-178, EBSCO Publishing, USA.

[15] L. Piancastelli, L. Frizziero. 2015. Multistage turbocharging systems for high altitude flight with common rail diesel engines. Asian Research Publishing Network. ARPN Journal of Engineering and Applied Sciences. ISSN 1819-6608, 10(1): 370-375, EBSCO Publishing, USA.

[16] L. Piancastelli, L. Frizziero. 2015. A new approach for energy recovery and turbo compounding systems for high altitude flight with common rail diesel engines. Asian Research Publishing Network. ARPN Journal of Engineering and Applied Sciences. ISSN 1819-6608, 10(2): 828-834, EBSCO Publishing, USA.

[17] L. Piancastelli, L. Frizziero. 2015. Mapping optimization for common rail diesel conversions from the automotive to the flying applications. Asian Research Publishing Network. ARPN Journal of Engineering and Applied Sciences. ISSN 1819-6608, 10(4): 1539-1547, EBSCO Publishing, USA.

[18] L. Piancastelli, L. Frizziero. 2015. GA based optimization of the preliminary design of an extremely high pressure centrifugal compressor for a small common rail diesel engine. Asian Research Publishing Network. ARPN Journal of Engineering and Applied Sciences. ISSN 1819-6608, 10(4): 1623-1630, EBSCO Publishing, USA.

[19] L. Piancastelli, L. Frizziero, G. Donnici. 2015. Common rail diesel-electric propulsion for small boats and yachts. Asian Research Publishing Network. ARPN Journal of Engineering and Applied Sciences. ISSN 1819-6608, 10(6): 2378-2385, EBSCO Publishing, USA.

[20] L. Frizziero, I. Rocchi. 2013. New finite element analysis approach. Published by Pushpa Publishing House. Far East Journal of Electronics and Communications. ISSN: 0973-7006, 11(2): 85-100, Allahabad, India.

[21] L. Piancastelli, L. Frizziero, E. Pezzuti. 2014. Kers applications to aerospace diesel propulsion. Asian Research Publishing Network. ARPN Journal of Engineering and Applied Sciences. ISSN 1819-6608, 9(5): 807-818, EBSCO Publishing, USA.

[22] L. Piancastelli, L. Frizziero. 2015. Diesel ecu mapping optimization for aircraft and helicopter applications. JP Journal of Heat and Mass Transfer. ISSN 0973-5763, 11(2): 151-167, Pushpa Publishing House, India.

[23] L. Piancastelli, L. Frizziero. 2015. Fuel consumption reduction and power downsize via robotized multiple speed gearbox and automatic selection system for an automotive application. JP Journal of Heat and Mass Transfer. ISSN 0973-5763, 12(2): 197-210, Pushpa Publishing House, India.

[24] L. Piancastelli, L. Frizziero, G. Donnici, G. Di Giacomo, A. Gatti. 2015. Optimized FSI flow simulation using modern up-to-date software systems: A direct comparison between simulated and tunnel results. Asian Research Publishing Network. ARPN Journal of Engineering and Applied Sciences. ISSN 1819-6608, 10(20): 807-818, EBSCO Publishing, USA.

[25] L. Piancastelli, R.A. Bernabeo, L. Frizziero. 2015. UAV remote control distraction prevention trough synthetic augmented virtual imaging and oculus rift-style headsets. Asian Research Publishing Network. ARPN Journal of Engineering and Applied Sciences. ISSN 1819-6608, 10(10): 4359-4365, EBSCO Publishing, 10 Estes Street, P.O. Box 682, Ipswich, MA 01938, USA.

[26] L. Piancastelli, L. Frizziero, 2015. Different approach to robust automatic control for airplanes. Asian Research Publishing Network. ARPN Journal of Engineering and Applied Sciences. ISSN 1819-6608, 10(6): 2321-2328, EBSCO Publishing, 10 Estes Street, P.O. Box 682, Ipswich, MA 01938, USA.

[27] L. Piancastelli, M. Forghieri, L. Frizziero, L. Chinni, M. Cremonini. 2015. Large HSDI CR diesel engines multiple injections and multiple swirls concept. Asian Research Publishing Network. ARPN Journal of Engineering and Applied Sciences. ISSN 1819-6608, 10(18): 7919-7928, EBSCO Publishing, 10 Estes Street, P.O. Box 682, Ipswich, MA 01938, USA.

[28] L. Piancastelli, A. Gatti, L. Frizziero, L. Ragazzi, M. Cremonini. 2015. CFD analysis of the Zimmerman's V173 stol aircraft. Asian Research Publishing Network. ARPN Journal of Engineering and Applied Sciences. ISSN 1819-6608, 10(18): 8063-8070, EBSCO Publishing, 10 Estes Street, P.O. Box 682, Ipswich, MA 01938, USA.

[29] L. Piancastelli, A. Castagnoli, L. Frizziero. 2015. Design and optimization of an aircraft propeller for tuned torsional vibration damping. Asian Research Publishing Network. ARPN Journal of Engineering and Applied Sciences. ISSN 1819-6608, 10(16): 6725-6731, EBSCO Publishing, 10 Estes Street, P.O. Box 682, Ipswich, MA 01938, USA.

[30] L. Piancastelli, A. Castagnoli, L. Frizziero, G. Donnici, S. Pica. 2015. Direct comparison of fsi optimized theodorsen and larrabee propellers. Asian Research Publishing Network, ARPN Journal of Engineering and Applied Sciences. ISSN 1819-6608, 10(16): 7250-7258, EBSCO Publishing, 10 Estes Street, P.O. Box 682, Ipswich, MA 01938, USA.

[31] L. Piancastelli L., Frizziero G. Donnici. 2015. Common rail diesel - Automotive to aerial vehicle conversions: An update (Part I). Asian Research Publishing Network. ARPN Journal of Engineering and Applied Sciences. ISSN 1819-6608, 10(6): 2479-2487, EBSCO Publishing, 10 Estes Street, P.O. Box 682, Ipswich, MA 01938, USA.

[32] L. Piancastelli, L. Frizziero, A. Rotondi. 2015. Optimum installation of a common rail diesel engine on a “classical” helicopter: The UH1. JP Journal of Heat and Mass Transfer. 12(1): 45-64, 2015.

[33] L. Piancastelli, L. Frizziero, G. Donnici. 2015. A new concept for low inertia electric turbocompounding in racing spark ignition engines. JP Journal of Heat and Mass Transfer. 12(1): 1-14.

[34] L. Piancastelli, L. Frizziero. 2015. Preliminary optimization of a common rail direct injection diesel alternative to the AE2100 class turboshafts. Asian Research Publishing Network. ARPN Journal of Engineering and Applied Sciences. ISSN 1819-6608, 10(11): 4738-4747, EBSCO Publishing, 10 Estes Street, P.O. Box 682, Ipswich, MA 01938, USA.

[35] L. Frizziero, I. Rocchi, G. Donnici, E. Pezzuti. 2015. Aircraft diesel engine turbocompound optimized. JP Journal of Heat and Mass Transfer. 11(2): 133-150.

[36] L. Piancastelli, L. Frizziero, G. Donnici. 2015. The meredith ramjet: An efficient way to recover the heat wasted in piston engine cooling. Asian Research Publishing Network. ARPN Journal of Engineering

and Applied Sciences. ISSN 1819-6608, 10(12): 5327-5333, EBSCO Publishing, 10 Estes Street, P.O. Box 682, Ipswich, MA 01938, USA.

[37] L. Piancastelli, L. Frizziero, G. Donnici. 2015. Common rail diesel - automotive to aerial vehicle conversions: An update (Part II). Asian Research Publishing Network. ARPN Journal of Engineering and Applied Sciences. ISSN 1819-6608, 10(8): 3286-3294, EBSCO Publishing, 10 Estes Street, P.O. Box 682, Ipswich, MA 01938, USA.

[38] L. Piancastelli, L. Frizziero, G. Donnici. 2015. Common rail diesel - automotive to aerial vehicle conversions: An update (Part III). Asian Research Publishing Network. ARPN Journal of Engineering and Applied Sciences. ISSN 1819-6608, 10(14): 5823-5830, EBSCO Publishing, 10 Estes Street, P.O. Box 682, Ipswich, MA 01938, USA.

[39] L. Piancastelli, L. Frizziero, S. Marcoppido, E. Pezzuti, “Feasible optimum design of a turbocompound diesel brayton cycle for diesel-turbo-fan aircraft propulsion” edizioni ETS, “International Journal of Heat & Technology”, ISSN 0392-8764, Volume 30, n.2, pp. 121-126, Bologna 2012.

[40] L. Piancastelli, N. E. Daidzic, L. Frizziero, I. Rocchi, “Analysis of automotive diesel conversions with kers for future aerospace applications” edizioni ETS, “International Journal of Heat & Technology”, ISSN 0392-8764, Volume 31, n.1, pp. 143-154, Bologna 2013.

[41] L. Piancastelli, L. Frizziero, G. Zanuccoli, N. E. Daidzic, I. Rocchi, “A comparison between cfrp and 2195-fsw for aircraft structural designs” edizioni ETS, “International Journal Of Heat & Technology”, ISSN 0392-8764, Volume 31, n.1, pp. 17-24, Bologna 2013.

[42] L. Piancastelli, L. Frizziero, E. Pezzuti, “Aircraft diesel engines controlled by fuzzy logic”, Asian Research Publishing Network (ARPN), “Journal of Engineering and Applied Sciences”, ISSN 1819-6608, Volume 9, Issue 1, pp. 30-34, 2014, EBSCO Publishing, 10 Estes Street, P.O. Box 682, Ipswich, MA 01938, USA.

[43] L. Piancastelli, L. Frizziero, E. Morganti, E. Pezzuti: “Method for evaluating the durability of aircraft piston engines”, Published by Walailak Journal of Science and Technology The Walailak Journal of Science and Technology, Institute of Research and Development, Walailak University, ISSN: 1686-3933, Thasala, Nakhon Si Thammarat 80161, Volume 9, n.4, pp. 425-431,Thailand, 2012.

[44] L. Piancastelli, L. Frizziero, E. Morganti, A. Canaparo: “Fuzzy control system for aircraft diesel engines” edizioni ETS, “International Journal of Heat & Technology”, ISSN 0392-8764, Volume 30, n.1, pp. 131-135, Bologna 2012.

[45] L. Piancastelli, L. Frizziero, E. Pezzuti, “Kers applications to aerospace diesel propulsion”, Asian Research Publishing Network (ARPN), “Journal of Engineering and Applied Sciences”, ISSN 1819-6608, Volume 9, Issue 5, pp. 807-818, 2014, EBSCO Publishing, 10 Estes Street, P.O. Box 682, Ipswich, MA 01938, USA.

[46] L. Piancastelli, L. Frizziero, I. Rocchi, G. Zanuccoli, N. E. Daidzic, “The “C-triplex” approach to design of CFRP transport-category airplane structures” edizioni ETS, “International Journal of Heat & Technology”, ISSN 0392-8764, Volume 31, n.2, pp. 51-59, Bologna 2013.

[47] L. Frizziero, I. Rocchi. 2013. New finite element analysis approach. Published by Pushpa Publishing House. Far East Journal of Electronics and Communications. ISSN: 0973-7006, 11(2): 85-100, Allahabad, India.

VOL. 11, NO. 7, APRIL 2016 ISSN 1819-6608
ARPN Journal of Engineering and Applied Sciences

www.arpnjournals.com

Symbols

Symbol	Description	Unit	Value
p	Static pressure	Pa	-
p_b	Basic static pressure	Pa	22,632.1
T_b	Basic temperature	K	216.65
H_b	Basic altitude	m	11,000
p_0	Sea level pressure	Pa	101,325
Boost	Manifold pressure	Pa	-
H	Altitude	m	-
g_0	Gravity acceleration	m/s^2	-
R	Ideal gas constant	m^3Pa/K	287.053
r_{inlet}	Inducer pressure ratio	-	-
CFR	Corrected Flow Rate	lb/min	-
ρ	Air density	kg/m^3	-
V_{cc}	Engine displacement	cc	-
rpm	Crankshaft velocity	rpm	-
η_e	Volumetric efficiency	-	-
τ	=1 for 2 stroke, =2 for 4 stroke	-	-
T_r	Inlet temperature	F abs	-
$p_{0\ psi}$	Inlet pressure	psi	-
BFR	Basic Flow Rate	lb/min	-
$BVFR_m$	Basic Volumetric Flow Rate	m^3/s	-
rps	Crankshaft velocity	rps	-
$\overline{p_{intake}}$	Intake pressure	Pa	-
ρ_{intake}	Intake air density	kg/m^3	
T_{intake}	Intake air temperature	K	-
BFR_m	Basic Mass Flow Rate	kg/s	-
$CBVFR_m$	Corrected Basic Volumetric Flow Rate	m^3/s	-
ρ_{OA}	Outside Air density	kg/m^3	-
p_{OA}	Outside Air static pressure	Pa	-
T_{OA}	Outside Air Temperature	K	-
$boost_{nb}$	Equivalent boost	Pa	
T_{boost}	Air Temperature after aftercooler	K	323.15
T_0	Sea level temperature for engine tests	K	293.15
r_{nb}	Equivalent pressure ratio	-	-
T_r	Exit temperature compressor	K	-
T_{intake}	Intake temperature engine	K	-
T_r	Inlet temperature compressor	K	-
PR_i	Pressure ratio compressor	-	-
η_c	Compressor efficiency	-	-
$PR_{singlestage}$	Pressure ratio single stage		
P_{lstage}	Pressure after low pressure stage	Pa	
PR	Pressure ratio	-	-
$\rho_{Garrett}$	Garrett reference air density	kg/m^3 $lb/feet^3$	1.105 0.069
$\rho_{intermediate}$	Intermediate stage compressor air density	kg/m^3	-
p_{20000}	Static pressure at	Pa	5,474.89